



Diffusion kurtosis imaging provides quantitative assessment of the microstructure changes of disc degeneration: an in vivo experimental study

Li Li¹ · Zhiguo Zhou² · Jing Li³ · Jicheng Fang¹ · Yuanyuan Qing¹ · Tian Tian¹ · Shun Zhang¹ · Gang Wu¹ · Alessandro Scotti⁴ · Kejia Cai⁴ · WenZhen Zhu¹

Received: 8 February 2018 / Revised: 8 February 2019 / Accepted: 12 February 2019 / Published online: 18 February 2019
© Springer-Verlag GmbH Germany, part of Springer Nature 2019

Abstract

Objective Our aim was to assess the microstructural changes of intervertebral disc degeneration induced by annulus needle puncture in rats by diffusion kurtosis imaging (DKI).

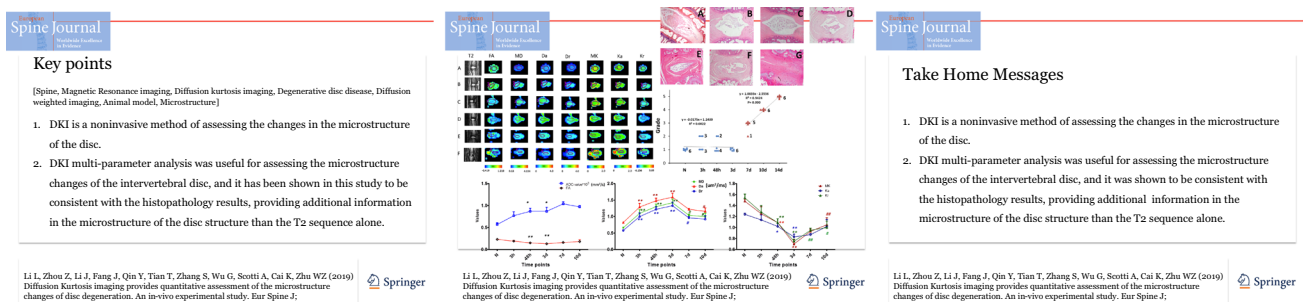
Methods Eighteen rats (36 discs) were punctured percutaneously at the intervertebral disc between C6/7, C7/8 (C-coccygeal vertebrae) with a 21-gauge needle. The rats were divided into six groups according to the time after the puncture: 3 h, 48 h, 3 days, 7 days, 10 days and 14 days. There were six discs in three rats in the control group. The rats' tail was imaged at 3T MRI with T₂-weighted and diffusion-weighted and diffusion kurtosis imaging (DWI)/DKI sequences. The discs were categorized using a five-grade degeneration system based on the T₂ images. The height of the discs and the parameters in DWI/DKI were measured and compared between the different time points. The histological images were also obtained from the discs.

Results The histological study revealed that the discs in the rat of the punctured groups were degenerated. The T2 grades of different groups presented an increasing trend from 7 to 10 days after puncture ($R^2 = 0.9424$, $P < 0.001$), while the DWI/DKI parameters changes were consistent with the histological changes at the different time points and showed significant differences between the different groups ($P < 0.05$).

Conclusions DKI provides quantitative assessment of the microstructure changes of disc degeneration, and it is a non-invasive method. The DKI multi-parameter analysis is sensitive to discs changes caused by puncture.

Graphical abstract

These slides can be retrieved under Electronic Supplementary Material.



Keywords Spine · Magnetic resonance imaging · Diffusion kurtosis imaging · Degenerative disc disease · Diffusion-weighted imaging · Animal model · Microstructure

Electronic supplementary material The online version of this article (<https://doi.org/10.1007/s00586-019-05924-3>) contains supplementary material, which is available to authorized users.

Extended author information available on the last page of the article

Introduction

Degenerative disc disease (DDD) is considered to be one of the major causes of low back pain. In the intervertebral disc degeneration, the morphology, biochemistry and biomechanics of the intervertebral discs have undergone a series of complex and continuous changes, leading to the loss of the disc function [1]. With the development of new technologies and materials, many innovative methods for repairing discs have been proposed. To test the reliability of these new methods, animal experiments were usually used [2]. However, according to one of the theories of intervertebral disc degeneration mechanism—“Degeneration of the disc was caused by mechanical injury,” the percutaneous disc puncture model of rat caudal vertebra is the most commonly used animal model for testing these novel potential therapies [1, 3–7].

Diffusion-weighted imaging (DWI) is a magnetic resonance imaging method that measures the diffusion properties of water molecules. In its most widespread form of usage, it assumes a Gaussian diffusion model, but many variations of the technique can also probe the non-Gaussian diffusion characteristics. Among the latter, diffusion kurtosis imaging (DKI) has been widely used for detection of microstructural tissue changes and grading diagnosis (in brain diseases, breast lesions, hepatocellular carcinoma and other disease) [8–13]. Multiple parameters can be extracted from DKI analysis, including fractional anisotropy (FA), mean diffusivity (MD), axial diffusivity (Da), radial diffusivity (Dr), mean kurtosis (MK), axial kurtosis (Ka) and radial kurtosis (Kr). The FA value is a measure of microstructural directionality, and it is dependent on the orientation and number of cells and the accessibility to the extracellular space. The MD value is sensitive to the diffusion of water molecules in the tissue, while the MK value is thought to be related to the microstructure complexity and density [14]. The Da and Dr values are the values of diffusivity in axial and vertical directions respectively, while the Ka and Kr values are the corresponding values of kurtosis in those directions.

In a previous study [15], it has been found that apparent diffusion coefficient (ADC) and DKI can show differences in the microstructure of the intervertebral disc between sexes in normal rats. Also, DKI revealed microstructural differences on the nucleus pulposus in the intervertebral discs in grades 1 and 2. However, it is unclear whether DKI can show the differences in the microstructure of the intervertebral discs across different stages of degeneration. If that was the case, it could be used as a non-invasive probe to track the microstructure changes within the intervertebral discs during the degeneration process. In this study, T₂-weighted, DWI and DKI sagittal sections

were compared to histological measurements in the analysis of the microstructural changes in a rat punctured intervertebral disc degeneration model.

Methods

Animals

Twenty-six Sprague-Dawley rats (each weighing 250–300 g, female) aged 3 months were used in this study. The animals were purchased from the Experimental Animal Center. The animals were housed in an environment at 24 °C with humidity at 50%. The light cycle consisted of 12 h of daylight and darkness. All animal experiments were approved by the Ethics Committee on Animal Experimentation.

To get the precise statistical analysis [15], T₂-weighted sagittal sections were acquired covering the intervertebral discs between the sixth and seventh, seventh and eighth coccygeal (C) vertebrae (C6/7, C7/8) in the tail of all rats. A five-grade system modified from the classification proposed by Pfirrmann [16] was adopted to grade the discs degeneration based on the T₂ images. Rats were prescreened to accept only Grade 1 discs, so twenty-one rats were grouped as the discs being Grade 1 and subsequently divided into seven subgroups: one normal and six punctured groups. Each rat tail in the latter groups was punctured percutaneously at the intervertebral disc with a 21-gauge needle [17]. Before puncturing, X-rays were used to identify the target segment, and then the skin of the target segment was marked. The needle was positioned parallel to the endplates and inserted to the centre of the disc through the skin and annulus fibrosus, reaching into the nucleus pulposus with a depth of 5 mm from the skin. X-rays were then repeated to verify the proper positioning. Subsequently, the needle was turned 360 degrees around its axis and left in this position for 30 s before removal [18]. The six punctured groups were then divided according to the delay between the puncture and the imaging session: 3 h, 48 h, 3 days, 7 days, 10 days and 14 days. At each time point, the punctured discs were imaged using a 3T MRI before euthanasia, while the discs in normal group were imaged before the 3-h group.

Imaging protocol and reconstruction

MRI scans were performed using a 3-Tesla MR scanning system (*GE Discovery MR 750; GE Healthcare, Waukesha, WI, USA*) on all rats. A 3-cm-diameter surface receiver coil (*Chenguang, Shanghai, China*) was used to maximize image resolution and quality.

T₂-weighted sagittal sections

The settings of T₂-weighted sagittal sequence were as follows: fast spin-echo sequence with repetition time (TR) of 2000 ms and echo time (TE) of 36 ms; matrix: 256 × 256; rectangular field of view (FOV): 5.0 × 5.0 cm; voxel dimensions: 0.2 × 0.2 mm², slice thickness was 1 mm; interslice gap 1 mm.

DWI sagittal sections

DWI was performed with single-shot spin-echo EPI sequence (SS-EPI) and the following parameters: *b* value: 0, 1000 mm/s²; TR/TE = 2000/92 ms; matrix, 256 × 256; FOV, 11 × 11 cm; voxel dimensions: 0.4 × 0.4 × 0.03 mm³; gap = 0 mm.

DKI sagittal sections

The sagittal diffusion kurtosis images were collected with the acquisition parameters: TR/TE = 2500/96 ms; FOV, 11 × 11 cm; matrix, 256 × 256; voxel dimensions: 0.4 × 0.4 × 0.001 mm³; slice thickness = 1 mm; gap = 0 mm. The DKI protocol included two b₀ images and DW images

with two different *b* values (1250, 2500 mm/s²), each applied along 25 directions.

Imaging analysis

Two radiologists (8 years and 6 years' experience of imaging analysis and radiologic reading in MR imaging of the spine) assessed the MR data and graded the discs degeneration as previously described. The discs were blindly reviewed by them separately, and consistent results were reached after further discussion if needed. The disc height index (DHI) was also collected in the T₂-weighted sagittal images [19]. The vendor-supplied software (Advantage Workstation; version 4.6, GE Healthcare) was used to calculate the apparent diffusion coefficient (ADC) (mm²/s) value from the DWI images. The diffusion parameters derived from DKI included FA, MD, Da, Dr, MK, Ka and Kr. Mean values were computed by averaging the values within elliptic regions of interest (ROIs) which were 2–8 mm². To select the proper anatomical position for the measurement, the ROIs were drawn from the centre of the disc on the T₂-weighted sagittal images and then transposed on DWI and DKI images (Fig. 1) [15].

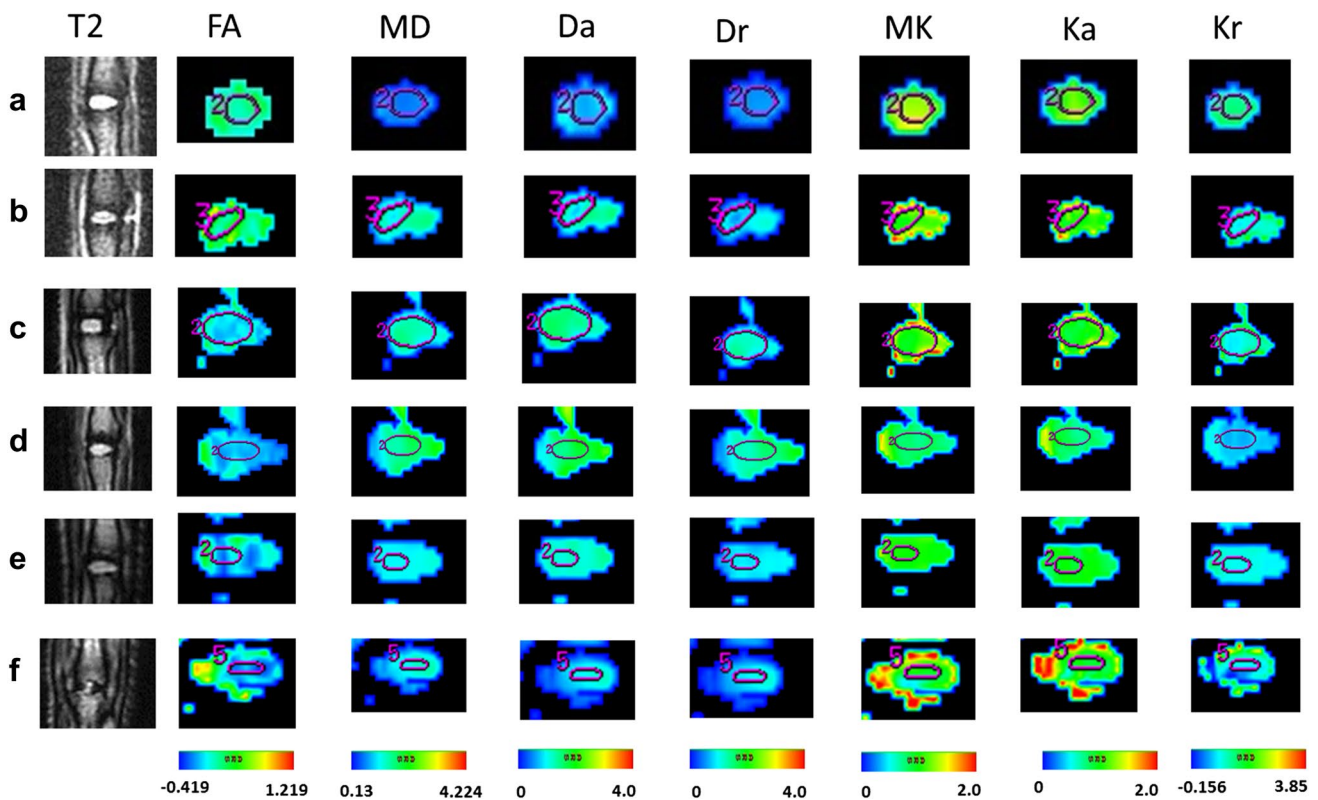


Fig. 1 T₂ images and DKI multi-parameter maps at different time points. From up to down: **a** normal; **b** 3 h; **c** 48 h; **d** 3 days; **e** 7 days; **f** 10 days. (Because the signal intensity of the intervertebral discs at

14 days was extremely weak in the T₂-weighted, DWI and DKI sagittal sections, there is no map.) The purple circles were the ROI of different parameters

Histological analysis

The rats in 3 h group were euthanized at 3 h after puncture, while the rats in 48-h group were euthanized at 48 h after puncture, and so on, for each of the groups (3 days, 7 days, 10 days and 14 days). The rats in normal group were euthanized at the same time with the 3-h group. The C6/7, C7/8 discs with adjacent vertebrae in all of the rats were harvested for histological examination. The spines were dissected carefully to avoid injury to the discs, fixed in 10% neutral buffered formalin and decalcified using Cal-Ex decalcifying solution HCL (Fisher Scientific, Fairlawn, NJ, USA). Specimens were then rinsed under running tap water and transferred to 75% ethanol. Subsequently, they were embedded in paraffin. The total processing time was about 13 h. Serial mid-sagittal slices from the mid-level of the intervertebral disc were cut with 5 μ m thickness by a microtome (Leica CM1520) and stained with haematoxylin and eosin [10]. Histological images were analysed under a microscope. To assess the stages of degeneration, a reference grading scale [20] was implemented by two observers blinded to the study.

Statistical analysis

The data were analysed using the SPSS statistics software package (IBM, ver. 23.0, Chicago, USA). The time dependence of T2 grades was examined based on linear regressions by ANOVA test. The Kruskal–Wallis test was applied to compare the differences in the DHI of the discs, ADC in DWI imaging and FA, MD, Da, Dr, MK, Ka, Kr in DKI between the different time points. Then, a ANOVA test with a post hoc test was used to test the multiple comparisons. The final data were presented as median \pm standard error (SE). *P* values smaller than 0.05 or 0.008 (when Bonferroni

correction was applied) were considered statistically significant.

Results

Histological changes after the puncture to the intervertebral disc at different time points

Figure 2 and Table 1 show the serial variations in the histology of the intervertebral disc after puncture.

Normal discs sections (Fig. 2a, Grade 4) presented with intact annulus fibrosus, a clear border between the annulus fibrosus and nucleus pulposus and a nucleus pulposus consisting of numerous uniformly distributed cells in the plump stroma.

At 3 h after puncture (Fig. 2b, Grade 8), the punctured site of the annulus fibrosus was visible, the annulus fibrosus became loose, the space between the annulus fibrosus and nucleus pulposus was enlarged, and the nucleus pulposus was shrunken. The intervertebral disc resulted therefore injured, and unevenly arranged enlarged cells with big water drops in which suggested oedema began to appear in the nucleus pulposus.

At 48 h after puncture (Fig. 2c, Grade 8), the annulus fibrosus got looser (especially the inner ring), the enlarged space between the annulus fibrosus and the nucleus pulposus increased, cavitation occurred, and the nucleus were moved to a side in the nucleus pulposus cells, and the matrix of the nucleus pulposus condensed.

At 3 days after puncture (Fig. 2d, Grade 10), the damages to the annulus fibrosus and nucleus pulposus were worse than those at 48 h, especially the loosening of the nucleus pulposus and the reduction in the stroma.

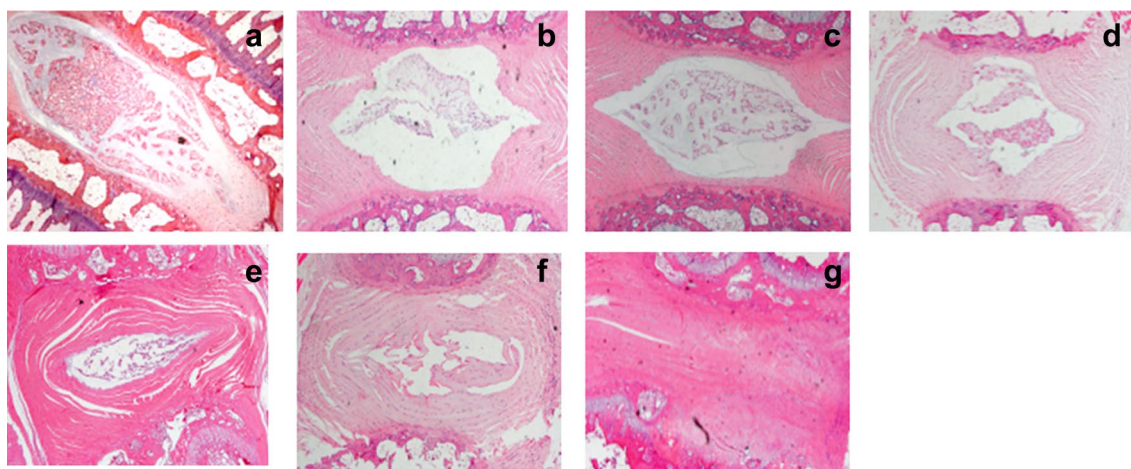


Fig. 2 Histological (H&E) staining images at different time points. **a** Normal; **b** 3 h; **c** 48 h; **d** 3 days; **e** 7 days; **f** 10 days; **g** 14 days

Table 1 The histological scores for each time point

Time points	Annulus fibrosus	Border between the annulus fibrosus and nucleus pulposus	Cellularity of the nucleus pulposus	Matrix of the nucleus pulposus	Grade
Normal	Normal fibrocartilage lamellae	Normal	Normal cellularity with large vacuoles in the gelatinous structure of the matrix	Normal gelatinous appearance	4
3 h	Ruptured patterned fibres in less than 30% of the annulus	Enlarged	Slight decrease in the number of normal cells and fewer vacuoles	Slight condensation of the extracellular matrix	8
48 h	Serpentined patterned fibres in less than 30% of the annulus	Enlarged	In the nucleus pulposus cells, cavitation occurred in the cells and moved the nucleus to a side	Slight condensation of the extracellular matrix	8
3 days	Serpentined patterned fibres in less than 30% of the annulus	Enlarged	Moderate in the number of cells and no vacuoles	Moderate condensation of the extracellular matrix	10
7 days	Serpentined patterned fibres in less than 30% of the annulus	Severe interruption	Severe decrease (50%) in the number of cells and no vacuoles	Severe condensation of the extracellular matrix	11
10 days	Serpentined patterned fibres in more than 30% of the annulus	Severe interruption	Severe decrease (50%) in the number of cells and no vacuoles	Severe condensation of the extracellular matrix	12
14 days	Serpentined patterned fibres in more than 30% of the annulus	None seen	Disappear	Disappear	12

Histological grading scale based on above four categories of degenerative changes with scores ranging from a normal disc with four points (one point in each category) to a severely degenerated disc with 12 points (three points in each category)

At 7 days after puncture (Fig. 2e, Grade 11), the loosening of the annulus fibrosus extended to the outer ring. The arrangement of the inner and outer ring in the annulus fibrosus was irregular. The cell became smaller, and the nucleus pulposus cell was pyknotic into band. The cytoplasm of the cells were concentrated. The stroma around the cells almost disappeared and was replaced by fibres.

At 10 days after puncture (Fig. 2f, Grade 12), the water-rich nucleus pulposus disappeared entirely and was replaced by disorganized fibres. Also, multinucleated giant cells were spotted among the fibres.

At 14 days after the puncture (Fig. 2g, Grade 12), the nucleus pulposus disappeared, the annulus fibrosus collapsed. Cracks and ruptures of collagen fibres could be seen in the annulus fibrosus.

Evaluation of T₂-based grades, DHI of the discs at different time points

The time dependence of T2 grades is shown in Fig. 3. There was an obviously linear correlation between the T2-based grades and time points from 7 days to 10 days after puncture ($R^2 = 0.9424, P = 0.000 < 0.001$), while there was no correlation from normal to 3 days after puncture. In addition, there was no significant group difference based on DHI.

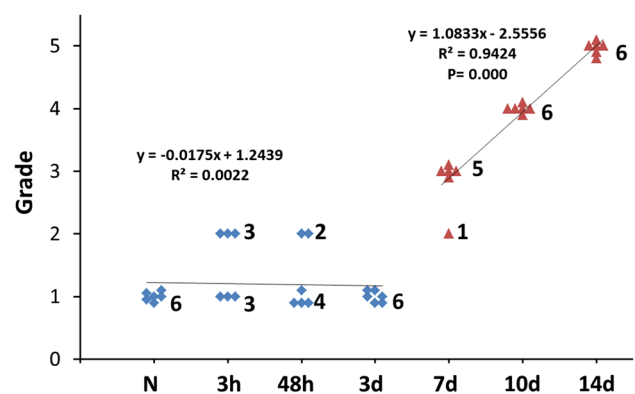


Fig. 3 The correlation between T2 grades and the time points based on linear regressions. The number beyond “red triangle” and “blue diamond” is the amount of the discs in the grade. From normal control to 3 days after puncture, there is no correlation between T2 grades and the time points. From 7 days to 14 days after puncture, there is an obviously linear correlation between T2 grades and the time points

Evaluation of the ADC value, DKI parameters of the discs at different time points

The analysis of ADC value, DKI parameters of the discs included the first six groups, but the last one (14 days after puncture) was excluded due to the extremely low signal

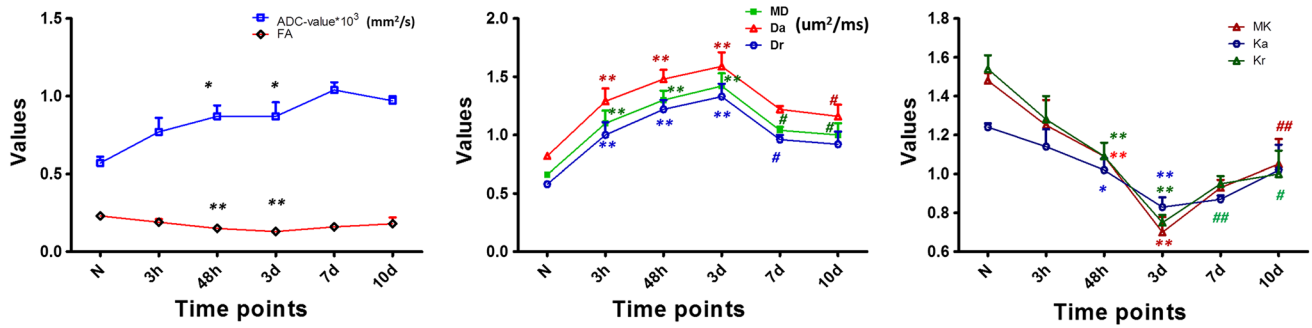


Fig. 4 Comparisons of ADC value, DKI parameters (FA, MD, Da, Dr, MK, Ka, Kr) among the groups at different time points. When significant differences compared to normal group are present:

* $P < 0.05$; ** $P < 0.008$; When significant differences compared to 3 days after puncture group are present: # $P < 0.05$; ## $P < 0.008$

intensity in the discs. The comparisons of imaging parameters among the different time points are summarized in Figs. 1 and 4.

Figure 4, Table 2 shows the quantitative analysis. Compared to the healthy group, all DKI parameters and ADC were significantly different in the groups (48 h and 3 days after puncture). At 3 h after puncture, the MD, Da and Dr values increased compared to those in the normal group ($P < 0.05$). At 48 h after puncture, the ADC, MD, Da and Dr values were even higher and the FA, MK, Ka and Kr values were significantly lower than normal and 3 h after puncture ($P < 0.05$). The variations peaked at 3 days and then reversed in the 7 days and 10 days after puncture where significant group differences in the MD, Da, Dr and Kr were recorded compared to the group of 3 days after puncture.

Discussion

The discs in groups of 3 h, 48 h and 3 days after the puncture were classified in the oedema period, while the discs in the groups from 7 to 10 days after the puncture were in

the fibrotic period. The DKI parameters are sensitive to the changes of the oedema period and fibrotic period, while T2 could distinguish the changes in fibrotic period.

The early degeneration process following disc puncture was not captured by the T2 grading. In the oedema period, the very presence of oedema could be a competing factor to T₂ signal loss due to the degeneration and the T₂ signal is unchanged. While in the fibrotic period, when the oedema likely reabsorbed, the T₂ signal increases. At 14 days after puncture, the T₂ grades were all Grade 5 (the most severe degeneration). These results are consistent with the ones presented by Issy's [4].

On the other hand, DWI and DKI parameters showed significant trends and changes within the nucleus pulposus at different time points (Fig. 4).

At 3 h after puncture, the MD, Da and Dr values increased compared to those in the normal group ($P < 0.05$). The MD, Da and Dr values are parameters describing the diffusion of water molecules [21]. When the space of the nucleus pulposus was enlarged, the diffusion of water molecules was easy and the MD values were increased. The Da and Dr values describe the degree of water molecule confinement in

Table 2 In different time points, the mean values of ADC value and DKI parameters

Parameters	State					
	Normal	3 h after puncture	48 h after puncture	3 days after puncture	7 days after puncture	10 days after puncture
ADC value (mm ² /s)	$(0.57 \pm 0.04) \times 10^{-3}$	$(0.77 \pm 0.09) \times 10^{-3}$	$(0.87 \pm 0.07) \times 10^{-3}$	$(0.87 \pm 0.09) \times 10^{-3}$	$(1.04 \pm 0.05) \times 10^{-3}$	$(0.97 \pm 0.03) \times 10^{-3}$
FA	0.23 ± 0.01	0.19 ± 0.02	0.15 ± 0.01	0.13 ± 0.01	0.16 ± 0.01	0.18 ± 0.04
MD (um ² /ms)	0.66 ± 0.02	1.10 ± 0.11	1.30 ± 0.08	1.42 ± 0.11	1.04 ± 0.03	1.0 ± 0.1
Da (um ² /ms)	0.82 ± 0.02	1.29 ± 0.11	1.48 ± 0.08	1.59 ± 0.12	1.22 ± 0.03	1.16 ± 0.1
Dr (um ² /ms)	0.58 ± 0.02	1.0 ± 0.11	1.22 ± 0.08	1.33 ± 0.11	0.96 ± 0.04	0.92 ± 0.11
MK	1.48 ± 0.04	1.25 ± 0.13	1.09 ± 0.07	0.70 ± 0.08	0.93 ± 0.04	1.05 ± 0.13
Ka	1.24 ± 0.02	1.14 ± 0.09	1.02 ± 0.06	0.83 ± 0.05	0.87 ± 0.02	1.02 ± 0.13
Kr	1.54 ± 0.07	1.28 ± 0.12	1.09 ± 0.07	0.75 ± 0.04	0.95 ± 0.04	1.0 ± 0.12

the vertical and parallel directions of the fibre, respectively. Their increase is consistent with the histological findings of the nucleus pulposus. Moreover, there was no statistic difference between ADC values at 3 h and normal. Therefore, the MD, Da and Dr resulted more sensitive than the ADC in detecting the oedema of the intervertebral disc nucleus.

The ADC, MD, Da and Dr values increased progressively, indicating that the changes of the intervertebral disc nucleus were getting worse, which was consistent with the pathological manifestations of histology. The MK value is thought to be related to the microstructure complexity and cellular density [14]. The reduction in the MK and Kr values indicated that the complexity or density of the microstructure was reduced. In addition, the FA value was also reduced, albeit not significantly, which might suggest the loss of the defined structures with proper directional anisotropy, and the extracellular space was enlarged. As a confirmation of these results, the histology showed the fibres inner loop getting loose, the nucleus pulposus cell density decreased and the extracellular matrix increased, which resulted in the expansion of the extracellular space of the nucleus pulposus. The changes in DWI parameters and DKI parameters were therefore consistent with all histological changes (increased oedema of the nucleus pulposus and reduction in matrix initiation).

The same process goes on at 3 days after puncture. ADC values were higher than those in the normal group, but were similar to 48 h after puncture. The MD, Da, and Dr values were higher than the normal group, which indicated again the worsening of the changes in the nucleus pulposus, consistently with the histological findings. The values of FA, MK, Ka and Kr were significantly lower than those in the normal group. The differences indicated that the expansion of the extracellular space was aggravated and the complexity and the density of the microstructure loosened.

At 7 days after puncture, the ADC, MD, Da and Dr values were significantly higher than those in normal group. However, the MD, Da and Dr values were lower than the oedema period (3 days after puncture), contrary to ADC values. This finding suggests that the oedema of the nucleus pulposus began to alleviate, which was in alignment with the histological findings. But, it is strange to find that ADC value was still increased, while the MD, Da and Dr values began to decrease. Maybe because DWI is a Gaussian diffusion model, DKI is a non-Gaussian diffusion model. Further study is needed to prove that. In line with this theory, the FA values were higher than those in the previous two periods, indicating a recovered directional microstructure. This in turn was consistent with histological changes (disappearance of the matrix which was replaced by fibre). The MK, Ka and Kr values followed the trend and resulted slightly higher than those at 3 days after puncture, but there was no significant difference ($P > 0.05$).

At 10 days after puncture, the MD, Da and Dr values decreased, compared with 3 days after puncture, indicating that cellular density changed and the oedema disappeared. The MK, Kr and Kr values increased, which indicated that the microstructure and density increased. Above all, all results were corresponding with the histological changes (the fibre increased). While there was no statistically significant difference compared with 3 h and 7 days after puncture, the trend was nonetheless clear.

In conclusion, according to the histopathology finding of the degeneration in this study, the diagnostic utility of DKI parameters was good in assessing the changes of the microstructure (water content, extracellular space, the density and the structure) in intervertebral disc, especially in the early stage.

A few short comings of this study are worth mentioning. This study only evaluated female rats, and our prior work showed gender differences in the rat model. Additionally, the process of pathological development in this rat model of intervertebral disc degeneration is not comparable to that of human discs. The process of disc degeneration is affected by many factors (ageing, gene, inadequate metabolite transport, etc.) [22, 23], and the exact pathological process still needs more research. What is certain is that water from the matrix is lost, while the proteoglycan diminishes with more fibrous appearing and cell changing in the nucleus pulposus [24]. The MD, Da and Dr are mainly indicative of the diffusion of water molecules, and their changes could reflect the loss of water in the degenerated discs. The FA value describes the directional anisotropy of the structures, while the MK, Ka and Kr values reveal changes in the tissue density and structure; thus, these four parameters can be indicative of the fibre deconstruction and reconstruction in the degenerated discs. Therefore, it is plausible that the multi-parameter analysis of DKI provides the markers of human intervertebral disc degeneration. We plan to further investigate on experimental models whether the sensitivity and specificity of these parameters are also maintained overtime. After that, we will focus on the possibility to apply the imaging protocol to the clinical practice.

Here, we demonstrated that DKI can distinguish the intervertebral disc microstructure differences between different stages of degeneration in the rat punctured intervertebral disc degeneration model.

Although the intervertebral disc degeneration model induced by Annulus needle puncture in rats was successfully developed and tested, further studies are needed with a model including a process of gradual loss of water. In future studies, the sample number will also be increased.

Conclusion

This study on punctured disc degeneration rat model demonstrated that DKI as a non-invasive method can be used to assess the changes in the microstructure of the disc. Particularly, our results support that the MD, Da and Dr values derived from DKI reflect water diffusion properties of the discs, FA indicates structural anisotropy, and the MK, Ka and Kr values correlate to nucleus pulposus density and other structure changes. DKI multi-parameter analysis has been proven to be useful for assessing the microstructural changes consistent with the histopathology results, providing additional information than the T₂ sequence alone.

Compliance with ethical standards

Conflict of interest None of the authors has any potential conflict of interest.

References

- Issy AC, Castania V, Castania M et al (2013) Experimental model of intervertebral disc degeneration by needle puncture in Wistar rats. *Braz J Med Biol Res* 46(3):235–244
- Yurube T, Hirata H, Kakutani K et al (2014) Notochordal cell disappearance and modes of apoptotic cell death in a rat tail static compression-induced disc degeneration model. *Arthritis Res Ther* 16(1):R31
- Silveira JW, Issy AC, Castania VA et al (2014) Protective effects of cannabidiol on lesion-induced intervertebral disc degeneration. *PLoS ONE* 9(12):e113161
- Issy AC, Castania V, Silveira JW et al (2015) Does a small size needle puncture cause intervertebral disc changes. *Acta Cir Bras* 30(8):574–579
- Inoue H, Montgomery SR, Aghdasi B et al (2015) The effect of bone morphogenetic protein-2 injection at different time points on intervertebral disk degeneration in a rat tail model. *J Spinal Disord Tech* 28(1):E35–E44
- Li D, Yang H, Huang Y, Wu Y, Sun T, Li X (2014) Lumbar intervertebral disc puncture under C-arm fluoroscopy: a new rat model of lumbar intervertebral disc degeneration. *Exp Anim* 63(2):227–234
- Han B, Zhu K, Li FC et al (2008) A simple disc degeneration model induced by percutaneous needle puncture in the rat tail. *Spine (Phila Pa 1976)* 33(18):1925–1934
- Iima M, Kataoka M, Kanao S et al (2018) Intravoxel incoherent motion and quantitative non-Gaussian diffusion MR imaging: evaluation of the diagnostic and prognostic value of several markers of malignant and benign breast lesions. *Radiology* 287(2):432–441
- Falk DA, Nilsson M, van Westen D, Falk DA (2018) Glioma grade discrimination with MR diffusion kurtosis imaging: a meta-analysis of diagnostic accuracy. *Radiology* 287(1):119–127
- Wang WT, Yang L, Yang ZX et al (2018) Assessment of microvascular invasion of hepatocellular carcinoma with diffusion kurtosis imaging. *Radiology* 286(2):571–580
- McClymont D, Teh I, Carruth E et al (2017) Evaluation of non-Gaussian diffusion in cardiac MRI. *Magn Reson Med* 78(3):1174–1186
- Ruan W, Zhong J, Guan Y et al (2017) Detection of smoke-induced pulmonary lesions by hyperpolarized 129 Xe diffusion kurtosis imaging in rat models. *Magn Reson Med* 78(5):1891–1899
- Shi RY, Yao QY, Zhou QY et al (2017) Preliminary study of diffusion kurtosis imaging in thyroid nodules and its histopathologic correlation. *Eur Radiol* 27(11):4710–4720
- Zhuo J, Xu S, Proctor JL et al (2012) Diffusion kurtosis as an in vivo imaging marker for reactive astrogliosis in traumatic brain injury. *Neuroimage* 59(1):467–477
- Li L, Zhu W, Chen W, Fang J, Li J (2017) The study of the intervertebral disc microstructure in matured rats with diffusion kurtosis imaging. *Magn Reson Imaging* 42:101–106
- Pfirrmann CW, Metzendorf A, Zanetti M, Hodler J, Boos N (2001) Magnetic resonance classification of lumbar intervertebral disc degeneration. *Spine (Phila Pa 1976)* 26(17):1873–1878
- Hsieh AH, Hwang D, Ryan DA, Freeman AK, Kim H (2009) Degenerative anular changes induced by puncture are associated with insufficiency of disc biomechanical function. *Spine (Phila Pa 1976)* 34(10):998–1005
- Li J, Guan H, Liu H et al (2017) Epoxyeicosanoids prevent intervertebral disc degeneration in vitro and in vivo. *Oncotarget* 8(3):3781–3797
- Keorochana G, Johnson JS, Taghavi CE et al (2010) The effect of needle size inducing degeneration in the rat caudal disc: evaluation using radiograph, magnetic resonance imaging, histology, and immunohistochemistry. *Spine J* 10(11):1014–1023
- Masuda K, Aota Y, Muehleman C et al (2005) A novel rabbit model of mild, reproducible disc degeneration by an annulus needle puncture: correlation between the degree of disc injury and radiological and histological appearances of disc degeneration. *Spine (Phila Pa 1976)* 30(1):5–14
- Zhang S, Zhu W, Zhang Y et al (2017) Diffusional kurtosis imaging in evaluating the secondary change of corticospinal tract after unilateral cerebral infarction. *Am J Transl Res* 9(3):1426–1434
- Adams MA, Roughley PJ (2006) What is intervertebral disc degeneration, and what causes it. *Spine (Phila Pa 1976)* 31(18):2151–2161
- Battié MC, Videman T (2006) Lumbar disc degeneration: epidemiology and genetics. *J Bone Joint Surg Am* 88(Suppl 2):3–9
- Roberts S, Evans H, Trivedi J, Menage J (2006) Histology and pathology of the human intervertebral disc. *J Bone Joint Surg Am* 88(Suppl 2):10–14

Publisher's Note Springer Nature remains neutral with regard to jurisdictional claims in published maps and institutional affiliations.

Affiliations

Li Li¹ · Zhiguo Zhou² · Jing Li³ · Jicheng Fang¹ · Yuanyuan Qing¹ · Tian Tian¹ · Shun Zhang¹ · Gang Wu¹ · Alessandro Scotti⁴ · Kejia Cai⁴ · WenZhen Zhu¹

✉ WenZhen Zhu
zhuwenzhen8612@163.com

¹ Radiological Department, Tongji Hospital, Tongji Medical College, HUST, Wuhan 430030, Hubei, People's Republic of China

² Department of Orthopedics, Wuhan Children's Hospital (Wuhan Maternal and Child Healthcare Hospital), Tongji Medical College, HUST, Wuhan 430030, Hubei, People's Republic of China

³ Department of Orthopaedic Surgery, Tongji Hospital, Tongji Medical College, HUST, Wuhan 430030, Hubei, People's Republic of China

⁴ Departments of Radiology, Department of Bioengineering, and the Center for MR Research, University of Illinois at Chicago, Chicago, IL, USA